



# Accounting for the spatial range of soil properties in pedotransfer functions

Shengping Wang<sup>a,b,c,\*</sup>, Peter Strauss<sup>b</sup>, Thomas Weninger<sup>b</sup>, Borbala Szeles<sup>c,d</sup>, Günter Blöschl<sup>c,d</sup>

<sup>a</sup> College of Hydraulic and Hydro-Power Engineering, North China Electric Power University, Beijing 102206, PR China

<sup>b</sup> Institute for Land and Water Management Research, Federal Agency for Water Management, A-3252 Petzenkirchen, Austria

<sup>c</sup> Institute of Hydraulic Engineering and Water Resources Management, Vienna University of Technology, Vienna, Austria

<sup>d</sup> Vienna Doctoral Programme on Water Resource Systems, Vienna University of Technology, Vienna, Austria

## ARTICLE INFO

Handling Editor: Budiman Minasny

### Keywords:

Pedotransfer function

Ensemble prediction

Spatial structure, uncertainty

## ABSTRACT

Pedotransfer functions (PTF) are widely used in soil hydraulic property modelling. Accounting for spatial structures of soil properties for improving the model performance of PTF is increasingly discussed. To understand how model performance varies when PTF are trained with samples of different spatial structure of the input data, we developed 12 ePTF (ensemble PTF) with data input from differently sized spatial domains to predict field capacity (FC) and wilting point (WP) of agriculturally used soils in Austria. The training domains generally had diameters equal to or larger than the spatial range of the explaining variables (bulk density BD, organic carbon content OC, Sand, Silt, and Clay) and the response variable (FC or WP). A stepwise regression technique was used to train the ePTF, and both bootstrap and random sampling were used to evaluate the uncertainties of the various ePTF. We found that, a training domain considerably larger than the spatial range of the input variables did not help develop a robust ePTF, particularly when applied on relatively larger scales, independent of their performances during the training stage. We conclude that, covering additional heterogeneous samples from outside of the spatial range of the input variables does not ensure an enhanced prediction capability of ePTF. Also, it might be worth paying more attention to the spatial structure of the predicted variable when its spatial range might be expected to be quite different from the predictors. This would have an implication for guiding sampling practices.

## 1. Introduction

Pedotransfer functions (PTF) commonly use readily available soil information to estimate soil physical or hydraulic properties (Rawls et al., 1982; Tietje and Tapkenhinrichs, 1993; Jian et al., 2021; Van Looy et al., 2017; Zhang et al., 2018; Zhang and Schaap, 2019; Sevastas et al., 2018). However, the application of PTF usually involves uncertainty of different types (Mayr and Jarvis, 1999; Chirico et al., 2010; Winter and Disse, 2010; Loosvelt et al., 2011, Achieng, 2019).

An number of studies were dedicated to revealing the shortcomings and uncertainties of PTF- prediction propagated into hydrological or environmental modelling (e.g. Guber et al., 2009; Deng et al., 2009; Chirico et al., 2010; Wösten et al., 2013; Sun et al., 2016; Blanco et al., 2018; Fatholouloumi et al., 2020; Kalumba et al., 2021). Also, whether and how the spatial structure of predicted variables are accounted for by PTF has been of increasing interest in relevant studies (Nemes et al., 2009; Liao et al., 2011; Jin et al., 2018; Dobarco et al., 2019; Szabo et al., 2019; Bourennane et al., 2021). This is because the stationarity

assumption does not guarantee that PTF properly simulate the spatial organization of predicted variables. Furthermore, predictions of PTF sometimes were found no spatial correlation with their corresponding observations at all (Milne et al., 2005; Pringle and Lark, 2006; Pringle et al., 2007; Chirico et al., 2007, 2010). Both Milne et al. (2005) and Pringle et al. (2007) used wavelet methods to evaluate the spatial structure of PTF prediction, suggesting that spatially non-correlated coefficients could not represent the spatial variance of observations at particular scales. Using geostatistical analysis tools, Liao et al. (2011) compared soil water observations with the predictions simulated by a few widely used PTF, suggesting that only some of the investigated PTF could simulate the spatial variation of investigated variables.

The previous studies all underline that established PTF should functionally perform well when reflecting the spatial variation of predicted variables, *i.e.* dependent variables. However, the results of previous studies on the importance of the spatial structure of inputs for developing PTF are ambiguous. Additionally, it is still unclear whether it is necessary to account for the spatial process of target variables in the

\* Corresponding author.

E-mail address: [Shengping\\_Wang@ncepu.edu.cn](mailto:Shengping_Wang@ncepu.edu.cn) (S. Wang).

training process to develop a robust PTF because a locally calibrated PTF may not be appropriate for predicting a target variable characterized by a large spatial correlation length (Pringle et al. 2007). Working on possible causes affecting PTF's performance and uncertainties, Finke et al. (1996) found that the model structure of PTF was less relevant in explaining the spatial variation of PTF predictions when compared with the spatial variability of input variables. Ye et al. (2007; 2008) suggested that uncertainties of PTF predictions could be significantly improved by considering the variance of co-kriging variables. Liao et al. (2014a) found that the input uncertainty had more influence on PTF prediction than parameter uncertainty. Deng et al. (2009) used co-kriging and bootstrapping to address spatial variability of inputs and parameter uncertainties, respectively, suggesting that using more training samples helped to reduce the uncertainty of parameter estimations in PTF development. Unlike the previously mentioned analysis, Chirico et al. (2007, 2010) suggested that PTF model structure was more influential in reducing the uncertainty than the spatial variability of the input dataset. They found it unnecessary to measure soil properties at a high spatial resolution when developing PTF, underlining the irrelevant role of the spatial structure of inputs affecting PTF performance.

In our analysis, instead of evaluating how PTF simulate spatial structures of target variables, we aimed to examine whether accounting for spatial structures of input variables (either predictors or predicted variables) significantly reduced errors in PTF predictions. We trained various PTF based on the samples from different spatial sizes of training domains. We hypothesized that it was possible to reduce PTF prediction errors by adequately accounting for the spatial range of inputs. Specifically, we aimed to i) understand how the performance of a PTF varied when the spatial range of the input variables was not correctly taken into account during training stage; and ii) reveal if the spatial range of a predicted variable was relevant to develop a robust PTF.

## 2. Data and methodology

### 2.1. Data availability

We used a datasets of the soil physical properties provided by the Federal Agency for Water Management, Institute for Land and Water Management Research, Austria, to develop PTF for predicting the field capacity (FC) and wilting point (WP) of soil. This extendible database contains information on soil samples collected over the last three decades. Soil samples were taken from different soil profiles mainly distributed within the agricultural production area of Austria. Since samples from deeper layers were unavailable for some soil profiles, only samples of the first two layers were considered during analysis. The first layer has an average sampling depth of  $15 \pm 9$  cm (i.e. the bottom depths of the sampling cylinders taken for analysis), whilst the second one has an average sampling depth of  $42 \pm 18$  cm. By default, a large number of soil physical and hydraulic parameters are measured for each soil sample. In this analysis, however, we only used soil texture (clay, sand, silt), bulk density (BD) and organic carbon (OC) as potential explanatory variables. FC and WP were obtained from the measurement of the retention curves. Soil texture was analyzed according to Austrian standards using the pipette method with  $\text{Na}_4\text{P}_2\text{O}_7 \cdot 10\text{H}_2\text{O}$  and  $\text{H}_2\text{O}_2$  (ÖNORM L 1061). Organic carbon was measured using wet or dry combustion (ÖNORM 1080, 1082). Bulk density was measured according to EN-ISO11272; for the measurement of retention curves, we used ISO11275. We used samples from 176 soil profiles in our analysis and established PTF for layers 1 and 2 respectively.

### 2.2. PTF development

Based on the kriging theory, we hypothesized that samples outside of the spatial range would induce more noise, leading to more uncertainty in the performance of PTF models. Thus, PTF accounting for the spatial structure of variables may perform better than those without accounting

for spatial structure. To test our hypothesis, we first estimated spatial correlation lengths of the input variables using the "gstat" procedure in R. Then, we specified several domains of diameters approximately equal to the correlation lengths of at least one variables. By using the samples from the various domains, we tried to investigate if and how PTF behaved when spatial structures of variables were taken into account.

The spatial distribution of the different samples for analysis of FC is displayed in Fig. 1. For the sake of brevity, we did not include the spatial distribution for parameter WP, which is almost identical to that of FC. Table 1 gives the estimated spatial ranges of the input variables according to the analysis of semivariogram (semivariograms may be found in the supplementary material 1). Table 2 shows the statistics of soil properties within the domains. ANOVA suggest that for most variables, there was no significant difference ( $p > 0.05$ ) among the training domains for either layer 1 or 2. However, when comparing the training domains with the application domains, most variables exhibited a significant difference for either layer 1 or 2.

### 2.3. Random sampling and bootstrapping

The number of samples involved in developing PTF differed between the specified domains (Table 2). This may interfere with identifying the role of the spatial structure of input variables. Therefore, for each training domain, sample subsets were generated by random sampling in R, with the number of the subset sampling equal to the number of samples available for the smallest domain. Following Nemes et al. (2010), random sampling for each domain was run 20 times. For each run, the derived subset of the sampling was subjected to stepwise linear regressions, with BD, OC, and soil texture as potential explanatory variables, and FC or WP as predicted variables. Accordingly, 20 PTF were derived for each domain.

In order to address parameter uncertainties of each PTF, bootstrapping was conducted using the "boot" package in R for deriving 1000 sets of bootstrapped coefficients for each PTF. In total, 20 x 1000 regression coefficients (herein we called bootstrapped PTF) were generated for each training domain, constituting ensemble PTF (ePTF). The ePTF were subsequently tested in the application domains (AD11 and AD12 for layer 1, and AD21, AD22, and AD23 for layer 2, respectively).

Random sampling combined with bootstrap allowed us to address both input uncertainty (i.e. the training dataset) and parameter uncertainty (i.e. the parameters of PTF) together.

### 2.4. Model evaluation and uncertainty analysis

In total, we obtained 12 ePTF for the specified training domains, among which  $ePTF_{FC,TD11}$ ,  $ePTF_{FC,TD12}$ ,  $ePTF_{FC,TD13}$ ,  $ePTF_{FC,TD21}$ ,  $ePTF_{FC,TD22}$ ,  $ePTF_{FC,TD23}$  were used for predicting FC of layer 1 and 2, whilst  $ePTF_{WP,TD11}$ ,  $ePTF_{WP,TD12}$ ,  $ePTF_{WP,TD13}$ ,  $ePTF_{WP,TD21}$ ,  $ePTF_{WP,TD22}$ ,  $ePTF_{WP,TD23}$  for predicting WP of layer 1 and 2, respectively. The two smallest training domains (i.e. TD11 and TD21) were not submitted to random sampling, so each one has only 1000 bootstrapped members that constitute their corresponding ePTF.

Following the method of Cichota et al. (2013), the arithmetic mean of the ensemble member predictions was considered the output of each ePTF. The average approach could reduce prediction uncertainty similarly to the others (Liao et al., 2014b). Three widely used criteria, root mean square error (RMSE<sub>ePTF</sub>), mean error (ME<sub>ePTF</sub>), and standard deviation error (SDE<sub>ePTF</sub>) (Schaap, 2004) were used to evaluate the performance of the ePTF in each domain (see equation (1) to (3)).

$$ME_{ePTF} = \frac{1}{N} \sum_{i=1}^N \left( \left( \frac{1}{M} \sum_{j=1}^M S_{ij} \right) - O_i \right) \quad (1)$$

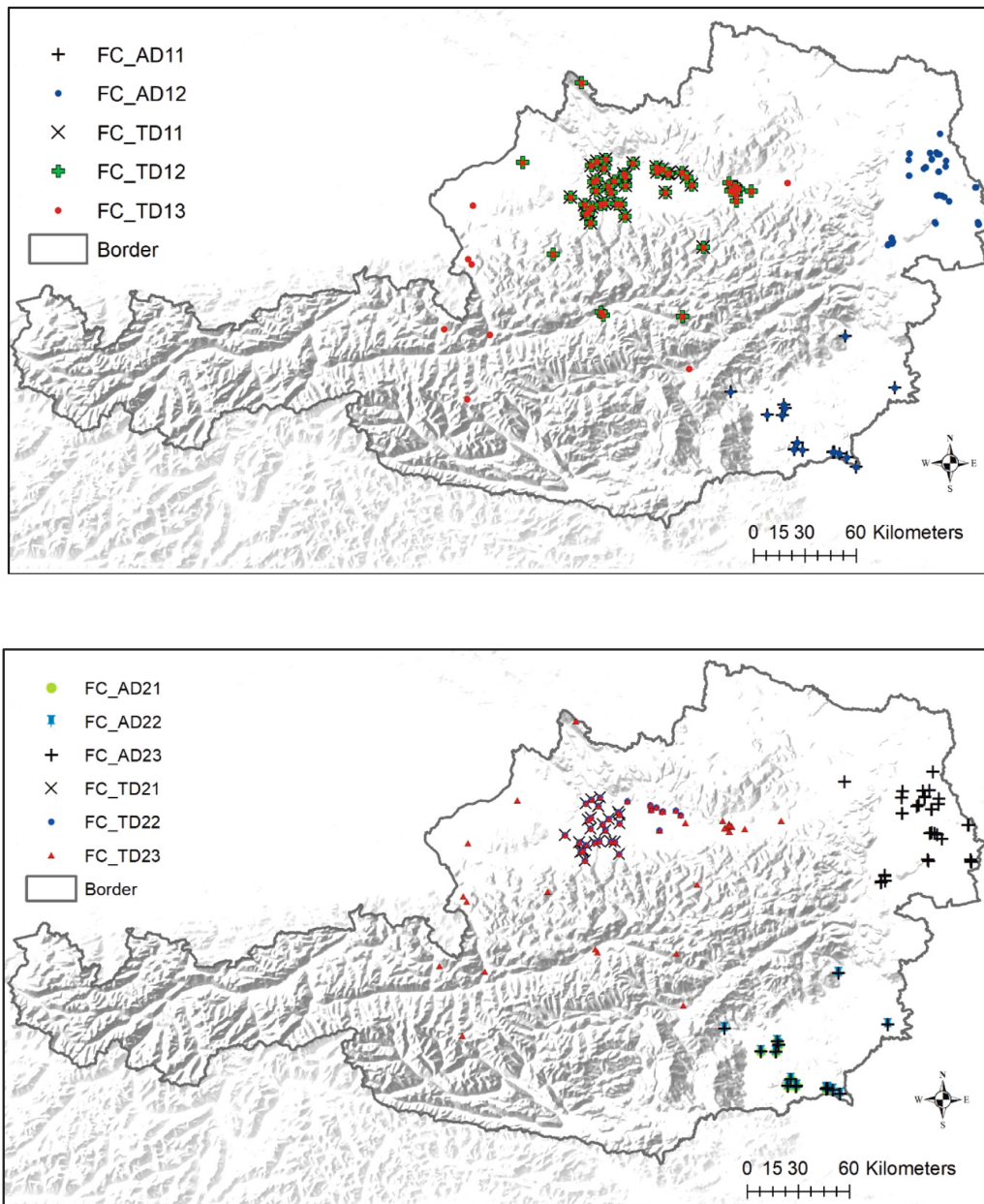


**Fig. 1.** Sampling distribution for developing PTF to estimate FC of a) layer 1 and b) layer 2, respectively. Different symbols denote the different training domains (TD11, TD12, TD13, TD21, TD22, TD23) and the application domains (AD11, AD12, AD21, AD22, AD23).

$$RMSE_{ePTF} = \sqrt{\frac{1}{N} \sum_{i=1}^N \left( \left( \frac{1}{M} \sum_{j=1}^M S_{ij} \right) - O_i \right)^2} \quad (2)$$

$$SDE_{ePTF} = \sqrt{\frac{1}{N-1} \sum_{i=1}^N \left( \left( \frac{1}{M} \sum_{j=1}^M S_{ij} \right) - O_i - ME_{ePTF} \right)^2} \quad (3)$$

where  $S_{ij}$  is the prediction of the  $j^{th}$  member PTF ( $j = 1, 2, \dots, M$ ) of the  $i^{th}$  soil sample ( $i = 1, \dots, N$ ),  $N$  represents the total number of soil samples within a specific domain, whilst  $M$  is taken as 40,000 or 20,000;  $O_i$  is the observation (FC or WP) for the  $i^{th}$  soil sample within the domains.  $ME_{ePTF}$  represents the mean prediction error of an ePTF performed in a specific domain, revealing an average tendency for overestimation or underestimation (DeVos et al., 2005; Nanko et al., 2014), and being an indicator of simulation accuracy of the investigated ePTF.  $RMSE_{ePTF}$  represents the overall performance of a specific ePTF (Chirico et al.,

2007), including both the accuracy error ( $ME_{ePTF}$ ) and the precision error represented as  $SDE_{ePTF}$  (Equation (3)). For a large  $N$ ,  $ME_{ePTF}^2 / RMSE_{ePTF}^2$  is usually considered the relative contribution of accuracy error to the total simulation error within a specified domain (Chirico et al., 2007).

To quantify uncertainties of the ePTF output, we estimated the distribution of the member PTF performances by using the average and the standard deviation of the performance values, denoted as  $\mu(RMSE)$  and  $\mu(ME)$ , and  $\sigma(RMSE)$  and  $\sigma(ME)$ , respectively.

$$\mu(RMSE) = \frac{1}{M} \sum_{j=1}^M RMSE_j \quad (4)$$

$$\mu(ME) = \frac{1}{M} \sum_{j=1}^M ME_j \quad (5)$$

**Table 1**  
Spatial range of the fitted semivariogram models for the variables potentially used in PTF.

Layer	Variables	Spatial range (km)
Layer 1	FC	210
	WP	180
	BD	113a;108b
	OC	—c
	Clay	—c
	Silt	175a; 161b
	Sand	183a;134b
Layer 2	FC	26
	WP	254
	BD	78a;109b
	OC	66a; 94b
	Clay	—c
	Silt	—c
	Sand	—c

a: estimated when the samples used for training PTF of FC were applied;  
b: estimated when the samples used for training PTF of WP were applied;  
c: No resultss because the fitting was not convergence or a singular model is derived.

$$\sigma(RMSE) = \sqrt{\frac{\sum_{j=1}^M (RMSE_j - \overline{RMSE})^2}{M - 1}} \quad (6)$$

$$\sigma(ME) = \sqrt{\frac{\sum_{j=1}^M (ME_j - \overline{ME})^2}{M - 1}} \quad (7)$$

where  $RMSE_j$  and  $ME_j$  represent the root mean square error and mean error, respectively, for the  $j^{th}$  member PTF of a specific domain.  $\overline{RMSE}$  and  $\overline{ME}$  are the means of the member performances for a specific domain. By investigating the patterns of the member performances, it is possible to reveal how the performances disperse around their mean values.

The PTF used to generate the member PTF differed in their explanatory variables due to the exclusion procedure of stepwise regression. Therefore, it was necessary to understand the difference in the explan-

**Table 2**  
Mean soil properties ( $\pm$ standard deviation) within the domains for training and application of PTF in layer 1 and 2.

		Training Domain			Application domain		
Layer 1	Domain Code_	TD11	TD12	TD13	AD11	AD12	
	Radius (km)	55	80	133	55	120	
	FC (%)	35.1 $\pm$ 4.6a*	35.4 $\pm$ 5.5a	36.1 $\pm$ 6.1a	33.0 $\pm$ 5.4c,a	27.9 $\pm$ 6.4d	
	WP (%)	17.3 $\pm$ 4.3a	17.4 $\pm$ 5.0a	17.5 $\pm$ 4.8a	18.3 $\pm$ 6.0c,a	15.7 $\pm$ 5.8d,a	
	BD ( $g \cdot cm^{-3}$ )	1.49 $\pm$ 0.11a	1.43 $\pm$ 0.16ab	1.42 $\pm$ 0.18b	1.42 $\pm$ 0.12c,ab,b	1.40 $\pm$ 0.12c,ab,b	
	OC (%)	1.15 $\pm$ 0.46a	1.55 $\pm$ 1.65ab	1.68 $\pm$ 1.68b	1.63 $\pm$ 0.52c,ab,b	1.48 $\pm$ 0.53c,ab,b	
	Clay (%)	22.1 $\pm$ 9.8a	21.3 $\pm$ 9.1a	20.8 $\pm$ 8.8a	18.3 $\pm$ 6.2c,a	17.9 $\pm$ 6.6c	
	Silt (%)	61.2 $\pm$ 12.5a	59.7 $\pm$ 13.2a	59.3 $\pm$ 13.3a	48.6 $\pm$ 15.6c	44.4 $\pm$ 15.2c	
	Sand (%)	16.7 $\pm$ 13.4a	18.9 $\pm$ 15.1a	19.8 $\pm$ 15.1a	33.1 $\pm$ 18.8c	37.6 $\pm$ 19.4c	
	Number of samples (N)	37 (36)**	68 (65)	76 (72)	21 (48)	68 (94)	
Layer 2	Domain Code_	TD21	TD22	TD23	AD21	AD22	AD23
	Radius (km)	25	40	133	25	55	120
	FC (%)	33.3 $\pm$ 6.64a	33.3 $\pm$ 7.37a	34.4 $\pm$ 7.11a	29.6 $\pm$ 9.4 cd,a	31.3 $\pm$ 9.1d,a	26.7 $\pm$ 8.1c
	WP (%)	17.4 $\pm$ 5.7a	17.1 $\pm$ 5.8a	17.2 $\pm$ 6.1a	18.5 $\pm$ 7.2 cd,a	19.4 $\pm$ 7.2d,a	15.6 $\pm$ 7.1c,a
	BD ( $g \cdot cm^{-3}$ )	1.51 $\pm$ 0.09a	1.50 $\pm$ 0.09a	1.46 $\pm$ 1.46a	1.53 $\pm$ 0.12c,a	1.52 $\pm$ 0.11c,a	1.45 $\pm$ 0.11d,a
	OC (%)	0.45 $\pm$ 0.32a	0.49 $\pm$ 0.31a	0.79 $\pm$ 0.57b	1.04 $\pm$ 0.53c	0.94 $\pm$ 0.56c	0.93 $\pm$ 0.57c,b
	Clay (%)	24.2 $\pm$ 10.3a	24.2 $\pm$ 11.5a	22.1 $\pm$ 10.9a	19.1 $\pm$ 7.9c,a	20.8 $\pm$ 8.9c,a	17.9 $\pm$ 8.4c
	Silt (%)	57.6 $\pm$ 11.9a	56.9 $\pm$ 12.8a	56.7 $\pm$ 13.5a	44.0 $\pm$ 18.0c	46.0 $\pm$ 17.6c	45.0 $\pm$ 15.9c
	Sand (%)	18.2 $\pm$ 18.2a	18.8 $\pm$ 18.8a	21.2 $\pm$ 18.6a	36.9 $\pm$ 24.3c	33.2 $\pm$ 23.9c	37.1 $\pm$ 21.6c
	Number of samples (N)	26 (26)	35 (35)	73 (70)	16 (30)	21 (45)	67 (90)

\*: Values with the same letter indicate insignificant differences ( $p > 0.05$ );

\*\* : Values in brackets refer to the numbers of samples used for developing PTFs of WP.

atory variables among the ePTF before assessing their performance for different domain sizes. We, thus, roughly quantified the relative importance of each predictor variable (relative importance of value or  $RIV_k$ ) of the ePTF by using equation ((8)–(10)),

$$RIV_k = \overline{RIV}_k \times w_k \quad (8)$$

$$\overline{RIV}_k = \frac{\sum_{l=1}^L RIV_{lk}}{N_k} \quad (9)$$

$$RIV_{lk} = \frac{t_{lk}}{\sum_{k=1}^K t_{lk}} \quad (10)$$

where  $RIV_k$  represents the relative contribution of the  $k^{th}$  variable ( $k = 1, 2, \dots, 6$ ) in the investigated ePTF;  $t_{lk}$  is the  $t$  value of variable  $k$  in a PTF  $l$  ( $l = 1, 2, \dots, 20$ ; for training domain TD11 and TD21,  $l = 1$ ), directly taken from the stepwise regression procedure, commonly representative of the relative importance of a variable in a model.  $N_k$  is the total times the  $k^{th}$  variable appears in 20 PTF;  $w_k$  is the weight of the  $k^{th}$  variable, taken as the  $N_k$  divided by 20.

### 3. Results

#### 3.1. Comparison of the developed ePTF

The developed ePTF did not all include the same predictors (Fig. 2) partly because of the excluding procedure of the stepwise regression technique. However, most ePTF, especially those from the larger domains, used most variables having spatial ranges as predictors, irrespective of their  $RIV_k$  values. For example, BD, Silt and Sand of layer 1, exhibiting a spatial range of 108, 161 and 134 km, respectively, were involved as predictors in ePTF<sub>WP,TD12</sub> and ePTF<sub>WP,TD13</sub> (See Fig. 2c), although their  $RIV_k$  values ranged from 0.01 to 0.04 only. BD and OC of layer 2 with a spatial range of between 78 and 109 and 66 and 84 km, respectively, were also included in the training ePTF<sub>FC,TD22</sub>, ePTF<sub>FC,TD23</sub> (Fig. 2b), and ePTF<sub>WP,TD23</sub> (Fig. 2d). A few training ePTF of small-sized domains did not use the variables having spatial range as the predictor variables. For example, the variable BD was not included in ePTF<sub>WP,TD11</sub> (Fig. 2c), even though BD exhibited a spatial range closed to the diameter of the domain TD11 of about 100 km around (Table 2). This failure to account for spatial structures of input variables in training PTF may have an unfavourable effect on model application or extrapolation.

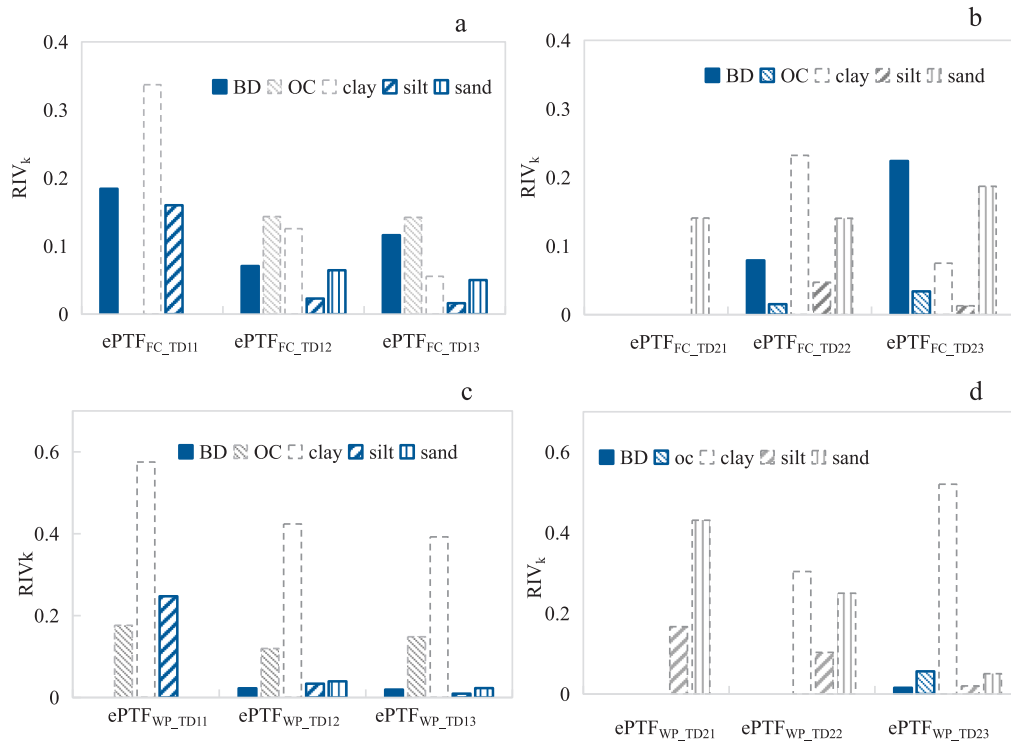


**Fig. 2.** RIV for the variables of the trained ePTF for layer 1 (a and c) and 2 (b and d). The ePTF of a) and b) are used for predicting FC, while the ePTF of c) and d) are used for predicting WP. Blue columns indicate variables with spatial range, grey columns denote variables without spatial range.

3.2. Performance of the ePTF during training stage.

3.2.1. FC

Performance of the trained ePTF to predict FC of layer 1 gradually declined as the size of the training domain increased. The best results were obtained from the smallest domain of TD11 (Fig. 3a), with RMSE<sub>ePTF</sub> and ME<sub>ePTF</sub> values being 2.94 and 0.06, respectively. The ePTFs from the other two domains (TD12 and TD13) performed differently, even though their soil properties were quite similar (Table 2), with RMSE<sub>ePTF</sub> values being 2.98 and 3.36, respectively (Fig. 3b and 3c). For layer 2, the best ePTF to predict FC was from the largest domain of

TD23 (Fig. 3f), with RMSE<sub>ePTF</sub> and ME<sub>ePTF</sub> being 3.35 and -0.19, respectively, generally better than ePTF of the other domains. Again, the similar soil properties between the training domains of TD22 and TD23 (Table 2) did not ensure a similar performances of the ePTF<sub>FC-TD22</sub> and ePTF<sub>FC-TD23</sub>.

3.2.2. WP

Unlike the ePTF for FC, the best ePTF to predict WP in both layers were all from the relatively small domains TD11 and TD22, with RMSE<sub>ePTF</sub> and ME<sub>ePTF</sub> being 2.53 and 0.02 for ePTF<sub>WP-TD11</sub> (Fig. 4a), and 2.70 and -0.26 for ePTF<sub>WP-TD22</sub> (Fig. 4e).

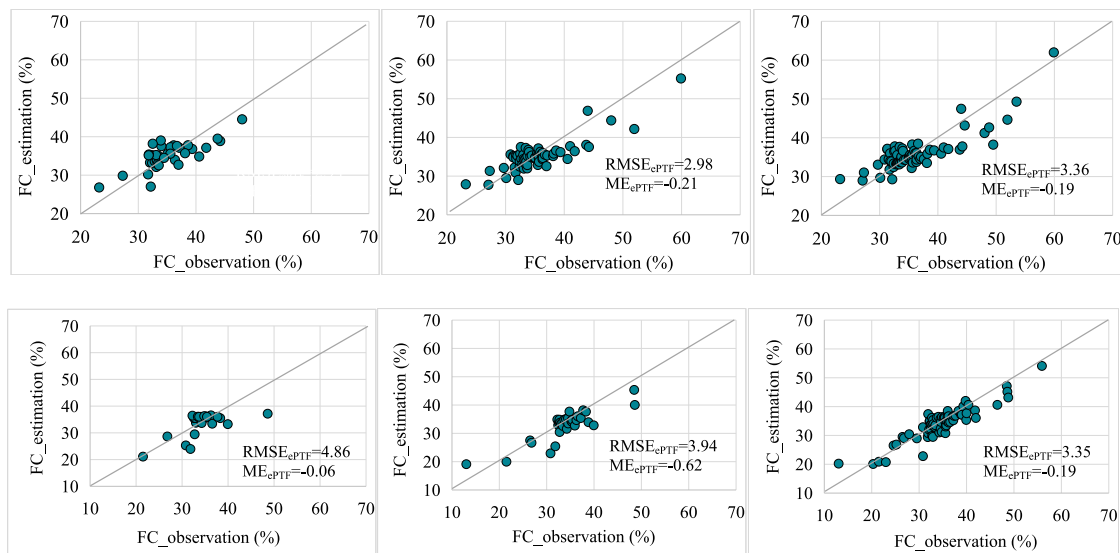


**Fig. 3.** Estimated FC from ePTF against their measurements within the training domains of layer 1: TD11 (a), TD12 (b), TD13 (c), and the training domains of layer 2: TD21 (d), TD22 (e), and TD23 (f), respectively. The points are representative of the samples within each specific domain. FC was estimated with ePTF<sub>FC-TD11</sub>, ePTF<sub>FC-TD12</sub>, ePTF<sub>FC-TD13</sub>, ePTF<sub>FC-TD21</sub>, ePTF<sub>FC-TD22</sub>, and ePTF<sub>FC-TD23</sub>, respectively.

### 3.3. Performance of the trained ePTF in the application domains

#### 3.3.1. Prediction of FC

The performance of the trained ePTF to predict FC of the application domains is given in Table 3. Interestingly, most of the well-performing ePTF during the training stage did not perform well during the application stage. For layer 1, the  $ePTF_{FC\_TD11}$  performed well in the application domain of AD11, better than the  $ePTF_{FC\_TD12}$  and  $ePTF_{FC\_TD13}$ . However, with increasing the size of the application domain (AD12), its performance declined considerably (Table 3). For layer 2, the best-performing  $ePTF_{FC\_TD23}$  during training stage did not excel in any of the three application domains. Instead, for the domains AD21 and AD22,  $ePTF_{FC\_TD22}$  was performing best, whilst it was  $ePTF_{FC\_TD21}$  in the largest domain AD23 (Table 3). Although most soil properties of the domain TD22, for example, the variables of OC, Silt, and Sand (Table 2), were different from those of AD21 and AD22, the  $ePTF_{FC\_TD22}$  from domain TD22 showed a robust prediction capability in the domains AD21 and AD22. While the soil properties differed between the domains TD21 and AD23, the  $ePTF_{FC\_TD21}$  performed well when it was applied to the application domain AD23.

#### 3.3.2. Prediction of WP

Similar to the prediction of FC, the ePTF that best predicted WP during the training stage did not perform best in either of the application domains (see Table 4). For layer 1, the  $ePTF_{WP\_TD11}$  did not behave as well as expected, although it had performed best during the training stage. Instead, the best-performing ePTF was  $ePTF_{WP\_TD13}$  in the application domain AD11, with  $RMSE_{ePTF}$  and  $ME_{ePTF}$  values of 4.49 and  $-1.07$  (Table 4). In the domain AD12, the  $ePTF_{WP\_TD12}$  behaved best, with  $RMSE_{ePTF}$  and  $ME_{ePTF}$  values of 4.16 and 0.30, respectively. For layer 2, the  $ePTF_{WP\_TD23}$  performed best in all three application domains, although this ePTF had a relatively poor performance during the training stage. The  $RMSE_{ePTF}$  of the  $ePTF_{WP\_TD23}$  in the domains AD21, AD22, and AD23 were 4.04, 4.65, and 4.14, and the  $ME_{ePTF}$  were  $-1.64$ ,  $-2.19$ , and 0.20, respectively (Table 4). Again, although most soil properties showed a significant difference between the training and the

application domains (Table 2), this did not impair the prediction capability of the ePTF at the application stage.

### 3.4. Uncertainty of the ePTFs predictions

#### 3.4.1. FC

Fig. 5 shows the ensemble members' performance patterns to predict FC. The ensemble members developed from layer 1 had  $\mu(RMSE)$  values ranging from 4.42 to 5.59 in the domain of AD11 (Fig. 5b), a magnitude similar to the one reported by Chirico et al. (2007). Whilst the domain of AD12 had the  $\mu(RMSE)$  values that ranged from 7.25 to 8.23 (Fig. 5b), indicating an increased prediction errors as the application domains expanded. The  $\sigma(RMSE)$  values of the ensemble members ranged from 0.50 to 1.06 in AD11, and 1.02 to 1.57 in AD12 respectively, all considerably smaller than the magnitudes of their corresponding  $\mu(RMSE)$  values, suggesting less uncertainty with their performances. Further looking into the sources of the errors of the performances, the prediction errors of the members in domain AD11 were mainly due to smaller precisions because the  $ME^2/RMSE^2$  values were lower than 0.1. In contrast, the larger domain AD12 exhibited accuracy errors that accounted for half of the total errors, with a  $ME^2/RMSE^2$  being 0.5 (Fig. 5c).

The  $\sigma(RMSE)$  value of the best performing  $ePTF_{FC\_TD11}$  in AD11 was 0.5, increasing by two times in AD12. In contrast, the  $ePTF_{FC\_TD12}$  had a  $\sigma(RMSE)$  value increase by 71% from AD11 to AD12. The differentiation of these uncertainties reveals the different prediction capabilities or the shortage of the two ePTFs in certain situations. We mainly ascribe the varying performance of the ePTF in the application domains to the degree to which the training ePTF accounted for the information on the spatial structure of variables. The variables BD, Silt, and FC of layer 1 exhibiting spatial ranges were involved as predictors of the  $ePTF_{FC\_TD11}$  (Fig. 2a). However, the  $ePTF_{FC\_TD11}$  was only trained with locally clustered samples of FC and Silt. This means that the training domain of TD11 was shorter than the spatial ranges of FC and Silt. The information about the spatial structure of both FC and Silt, thus, were not fully addressed in the ePTF. Therefore, the members of  $ePTF_{FC\_TD11}$  behaved

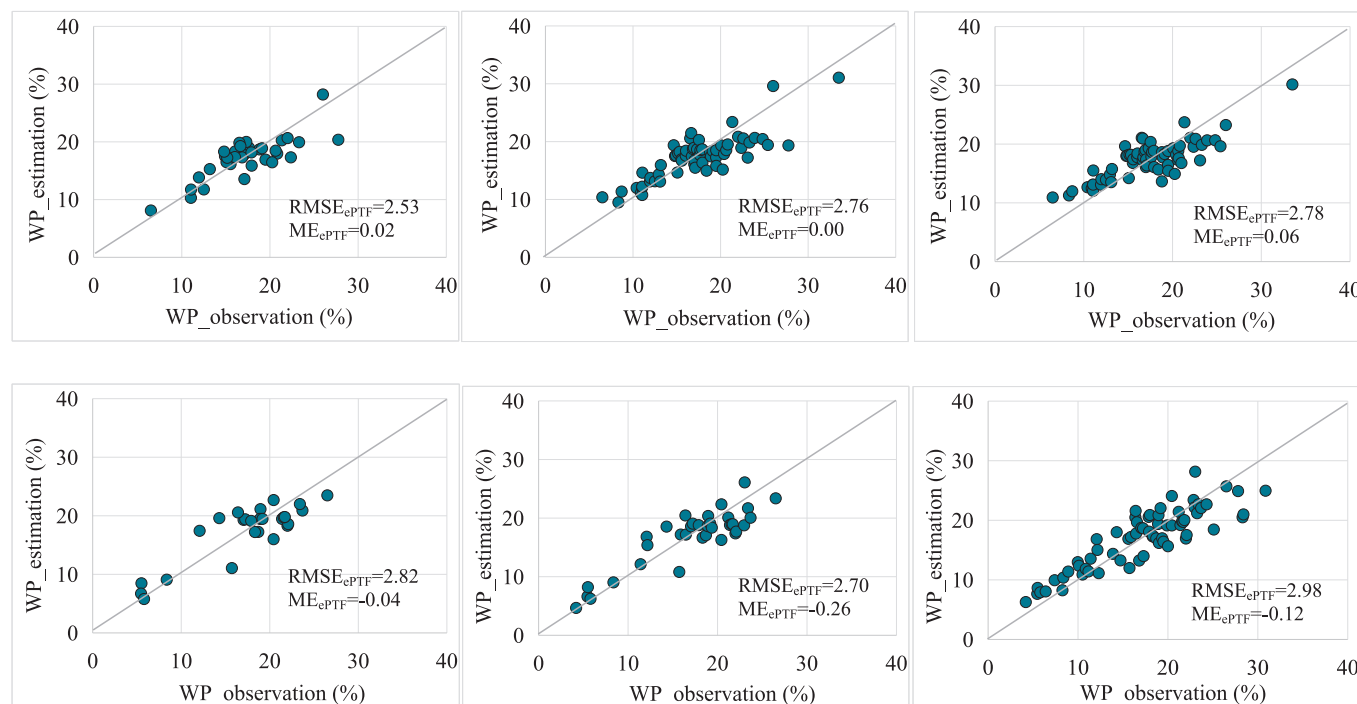


Fig. 4. Estimated WP from ePTF against their measurements within the training domains of layer 1: TD11 (a), TD12 (b), TD13 (c), and the training domains of layer 2: TD21 (d), TD22 (e), and TD23 (f), respectively. The points are representative of the samples within each specific domain. WP was estimated with  $ePTF_{WP\_TD11}$ ,  $ePTF_{WP\_TD12}$ ,  $ePTF_{WP\_TD13}$ ,  $ePTF_{WP\_TD21}$ ,  $ePTF_{WP\_TD22}$ , and  $ePTF_{WP\_TD23}$ , respectively.

**Table 3**  
Performance of the ePTF to predict FC of the application domains.

Layer 1	ePTF	AD11		AD12			
		RMSE <sub>ePTF</sub>	ME <sub>ePTF</sub>	RMSE <sub>ePTF</sub>	ME <sub>ePTF</sub>		
	ePTF <sub>FC_TD11</sub>	4.21	0.58	7.33	5.29		
	ePTF <sub>FC_TD12</sub>	4.49	0.64	7.06	5.12		
	ePTF <sub>FC_TD13</sub>	5.28	1.62	8.03	6.13		
Layer 2	ePTF	AD21		AD22		AD23	
		RMSE <sub>ePTF</sub>	ME <sub>ePTF</sub>	RMSE <sub>ePTF</sub>	ME <sub>ePTF</sub>	RMSE <sub>ePTF</sub>	ME <sub>ePTF</sub>
	ePTF <sub>FC_TD21</sub>	4.26	-1.01	4.73	-1.80	4.86	1.82
	ePTF <sub>FC_TD22</sub>	4.13	-0.79	4.25	-1.42	5.15	2.46
	ePTF <sub>FC_TD23</sub>	4.59	0.12	4.41	-0.63	7.09	4.43

**Table 4**  
Performance of the ePTF to predict WP of the application domains.

Layer 1	ePTF	AD11		AD12			
		RMSE <sub>ePTF</sub>	ME <sub>ePTF</sub>	RMSE <sub>ePTF</sub>	ME <sub>ePTF</sub>		
	ePTF <sub>WP_TD11</sub>	4.92	-1.93	4.23	-0.37		
	ePTF <sub>WP_TD12</sub>	4.57	-1.63	4.16	0.30		
	ePTF <sub>WP_TD13</sub>	4.49	-1.07	4.33	0.93		
Layer 2	ePTF	AD21		AD22		AD23	
		RMSE <sub>ePTF</sub>	ME <sub>ePTF</sub>	RMSE <sub>ePTF</sub>	ME <sub>ePTF</sub>	RMSE <sub>ePTF</sub>	ME <sub>ePTF</sub>
	ePTF <sub>WP_TD21</sub>	5.08	-3.43	5.86	-4.08	4.65	-1.83
	ePTF <sub>WP_TD22</sub>	5.08	-3.50	5.86	-4.13	4.62	-1.87
	ePTF <sub>WP_TD23</sub>	4.04	-1.64	4.65	-2.19	4.14	0.20

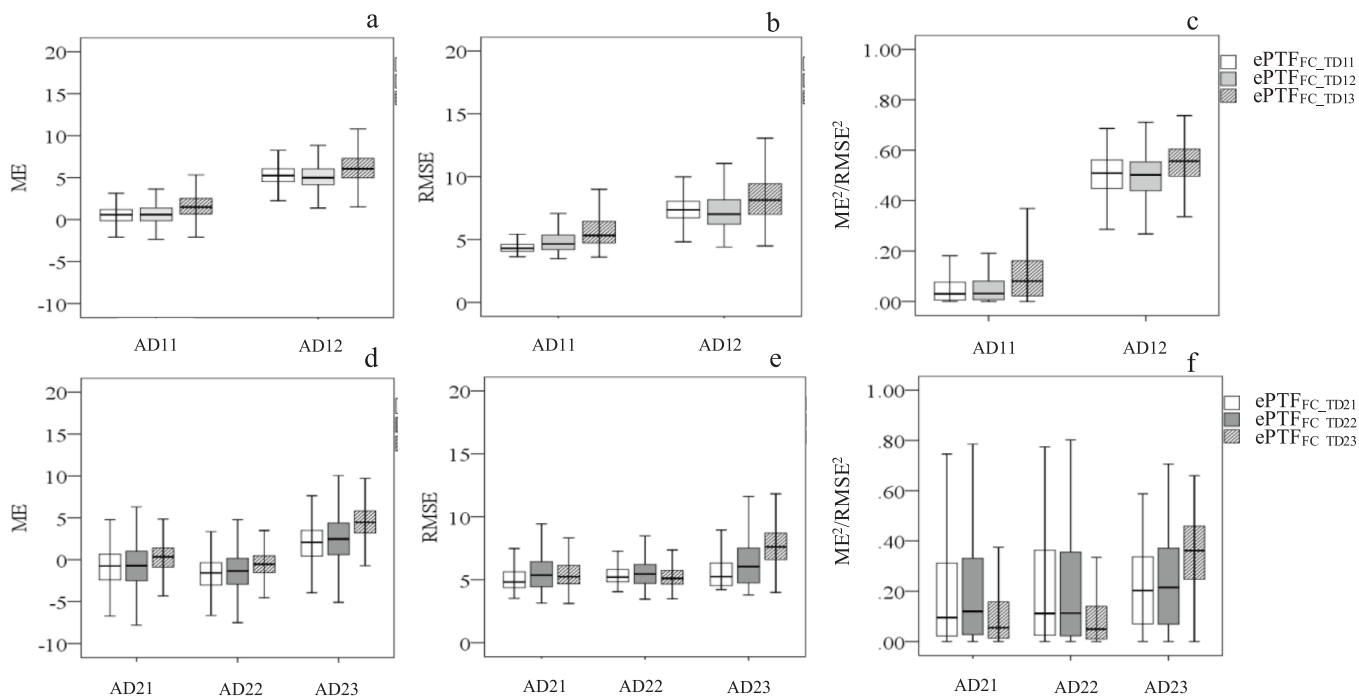


**Fig. 5.** Boxplots of the ePTF performance to predict FC in application domains of layer 1 (a, b, and c) and layer 2 (d, e, and f). Performance was evaluated in terms of ME (a,d), RMSE(b, e), and ME<sup>2</sup>/RMSE<sup>2</sup> (c,f).

better only when it was tested in a relatively small size domain AD11. The increased value of  $\sigma(RMSE)$  of the ePTF<sub>FC\_TD11</sub> ranging from 0.5 in AD11 to 1.0 in AD12 illustrates this defect of the ePTF when extrapolated into a large application domain.

The ePTF<sub>FC\_TD12</sub> includes most spatial variables (FC, BD,Silt, and Sand). Nevertheless, most training samples were from the domain with a diameter close to the spatial range of Silt, Sand and FC (160 km).

Therefore it possibly performed robustly, especially when applied to a relatively large testing domain (for example, AD12), where the requirement of accounting for the spatial structure of variables is more stringent to obtain an accurate spatial representation of soil properties (e.g. Pringle et al., 2007; Szabo et al., 2019; Bourennane et al., 2021). The small increase of  $\sigma(RMSE)$  value of ePTF<sub>FC\_TD12</sub> when altered from AD11 to AD12 confirmed its relative stable capability of extrapolation

compared to the  $ePTF_{FC\_TD11}$ . Dissimilarities of the dataset between the training and application domains were not mainly responsible for the performance of an ePTFs. More details will be given in section 4.2.

The ePTF to predict FC of layer 2 have showed less uncertainties (Fig. 5e), the  $\sigma(RMSE)$  values ranging from 1.04 to 1.84, considerably less than the magnitude of the  $\mu(RMSE)$  values ranging from 5.18 to 7.73. Both  $\mu(RMSE)$  and  $\sigma(RMSE)$  values of the  $ePTF_{FC\_TD21}$  were lower than those of the other ePTF in either of the domains, suggesting its robust prediction capability despite its worse performance during the training stage. Again, soil properties in terms of FC and Sand (the predicted variable and the predictor of the  $ePTF_{FC\_TD21}$ , respectively) were significantly different between the domain TD21 and the application domains AD21 and AD23 (Table 2). We mainly ascribe the robust performance of the ePTF to the fact that the diameter of the training domain of TD21 was close to the spatial range of FC (being 50 km and 25 km, respectively). Thus, the samples used for training the  $ePTF_{FC\_TD21}$  are representative of its spatial organization. It was noted that both BD and OC of layer 2 were not involved in training  $ePTF_{FC\_TD21}$  (Fig. 2b) even though they displayed apparent spatial ranges. This suggests that a sampling practice with only a small sampling domain was probably sufficient to deal with the issues of spatial variability, if a small spatial ranges characterized the target variable of a PTF. For  $ePTF_{FC\_TD22}$  and  $ePTF_{FC\_TD23}$ , most variables (i.e. FC, BD, and OC) exhibited spatial range and were involved in the training process (Fig. 2b). However, including sample data from outside of their spatial range is likely to expose their limits when the trained ePTFs were extrapolated to large size of domains. This is especially true for the  $ePTF_{FC\_TD23}$  because  $\mu(RMSE)$  and  $\sigma(RMSE)$  of this ePTF increased by 40% and 19%, respectively when the application domain expanded from AD21 to AD23.

### 3.4.2. WP

Similar to the results for FC, the ePTFs to predict WP of layers 1 and 2 also showed less uncertainty with  $\sigma(RMSE)$  values ranging between 0.32 and 0.75, which is considerably smaller than the magnitude of the  $\mu(RMSE)$  values of between 4.36 and 5.95 (Fig. 6). The main cause of

error for the ePTF of layer 1 was due to precision because the  $ME^2/RMSE^2$  ranged from 0.03 to 0.15 (Fig. 6c). In contrast, for layer 2, the accuracy error accounted for around half of the total errors in the domains AD21 and AD22. In the largest domain AD23, the precision error dominated the total errors (Fig. 6f). Among the ePTF of layer1, the  $ePTF_{WP\_TD13}$  performed best in the application domain of AD11, but it had a larger  $\sigma(RMSE)$  than the other ePTFs. Its performance decreased in the application domain AD12 (Fig. 6b). In contrast, the  $ePTF_{WP\_TD12}$  showed relatively stable performance, the  $\mu(RMSE)$  values in the domain AD11 and AD12 being 4.76 and 4.43, and the  $\sigma(RMSE)$  value decreasing by 40% when the domain changed from AD11 to AD12 (Fig. 6b). For layer 2, the  $ePTF_{WP\_TD23}$  consistently behaved well in all domains; its  $\sigma(RMSE)$  value outperformed the other ePTFs when the domain changed from AD21 to AD22 or to AD23 (Fig. 6e). This suggests a robust prediction capability of the ePTF.

These results suggest that the varied performance of the ePTF for predicting WP was mainly associated with the representativeness of the samples regarding the spatial structure of input variables. The relatively poor behaviour of the  $ePTF_{WP\_TD11}$  in either of the application domains of layer 1 was mainly due to the training sampling from the domain with a diameter of 100 km (See Table 2), considerably smaller than the domain of either Silt or WP, their spatial ranges being 160 ~ 180 km approximately (See Table 1). Thus, information about spatial structure of these variables was not fully addressed during training stage. In contrast, the members of  $ePTF_{WP\_TD12}$  used a training sample that correctly represented the apparent spatial organization (Fig. 2c), because the sampling diameter of the training domain TD12 (being around 160 km) were close to the spatial range (around 130 ~ 180 km) of most input variables (i.e. Silt, Sand, and WP). This led to a better performance of  $ePTF_{WP\_TD12}$  particularly when applied to a larger domain. As for the performance of  $ePTF_{WP\_TD13}$ , the training samples were partially located outside of the input variables' spatial range (WP, BD, Silt, and Sand, see Fig. 2c). This may be the reason for a decreasing performance when applied in a larger application domain. Compared with the other two ePTF, the relatively smaller errors of  $ePTF_{WP\_TD13}$  in

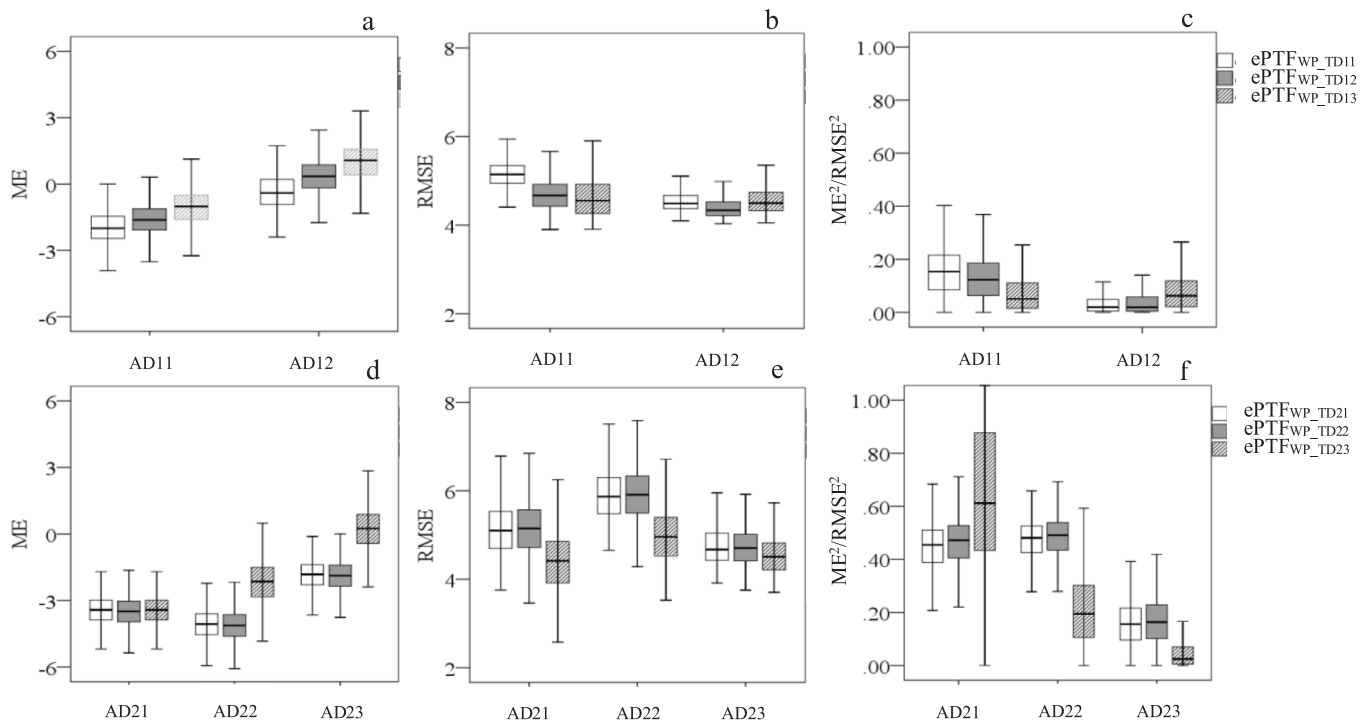


Fig. 6. Boxplots of the ePTF performance to predict WP in application domains of layer 1 (a, b, and c) and layer 2 (d, e, and f). Performance was evaluated in terms of ME (a,d), RMSE(b, e), and  $ME^2/RMSE^2$  (c, f).



the domain of AD11, in terms of  $ME^2/RMSE^2$  (0.07, see Fig. 6c), suggests that neglecting spatial structure may be only beneficial to improve the accuracy error in a small-scale application area, but not the precision error.

The sampling domain for  $ePTF_{WP\_TD23}$  had a diameter similar to the spatial range of WP, properly accounting for the spatial structure of WP. Therefore,  $ePTF_{WP\_TD23}$  outperformed  $ePTF_{WP\_TD21}$ ,  $ePTF_{WP\_TD22}$  for which the spatial structure of WP was not fully taken into account during training.

## 4. Discussion

### 4.1. Influence of potential processes or factors on examining the spatial structure of soil properties

Most PTF studies have commonly been carried out on hillslopes with a spatial resolution of the order of meters (Parker et al., 2012; Takagi and Lin, 2012; Martini et al, 2015). Terrain or topography effects on spatial organizations were often addressed in such analysis (Takagi and Lin, 2012; Tromp Van Meerveld and McDonnell, 2006). However, this does not imply that a regional scale analysis with coarse sampling density is not valid (Annabi et al., 2017). The spatial structure of most soil properties is usually controlled by several surface and subsurface processes or factors simultaneously, and these controls commonly exert their influences at different scales. For example, the spatial structure of soil organic carbon is often controlled by a climatic variation on the regional scale, while it is controlled by topographic factors on a hillslope scale (K. Yoo, et al., 2006). Soil texture of the surface or subsurface layer may be mainly controlled by terrain or topography effects on a field scale, whilst for deeper layers, it is mainly controlled by parent material on the regional scale (Ließ et al., 2012). For the case of soil moisture, Martini et al.(2015) and Takagi and Lin (2012) have shown that the spatial structure of soil moisture differed between layers, controlled by different processes at various scales. We thus assume that it is reasonable to investigate subsurface process and management controls on spatial structure of soil properties, although the sampling density has an order of magnitude of kilometers. Because most soil profiles of our analysis were mainly located in the agricultural production area, they are commonly featured with gentle slopes or flat topography. Thus, we assume that the terrain-controls on spatial organization of surface soil properties were also minimal. The examined soil properties in either layer 1 or 2 commonly exhibited a large spatial ranges (See Table 1), which has actually reinforced our assumptions.

### 4.2. Relevance of adequately addressing the spatial structure of soil properties in PTF development

In line with Pringle et al.(2007) and Deng et al. (2009), in which accounting for the spatial structure of soil properties was highlighted to improve the prediction capability of PTF, we found that  $ePTF$  could perform well if they were trained with the samples from domains that are characterized by their diameters approximately equal to the spatial range of soil properties. This was independent of their performance during the training stage. Whilst more and more analysis paid attention to increasing sampling density and extending sampling domains using novel sensing techniques (e.g. Van Looy et al., 2017; Loiseau et al., 2019; Pinnington et al., 2021), we found that covering more additional heterogeneous samples to train  $ePTF$  did not guarantee to enhance the precision of the predictions. This is because total prediction errors increased and the performance decreased accordingly, especially when  $ePTF$  were applied to a relatively large application domain. Several of our  $ePTF$  illustrate the interference of heterogeneous information on their performance. For example, the  $ePTF_{FC\_TD13}$  took into account all the spatial variables (including BD, Silt, Sand, and FC) in the training process. However, the spatial range of these soil properties (approximately 112 ~ 209 km) was considerably smaller than the training

domain TD13 with 266 km which affected the  $ePTF_{FC\_TD13}$  and decreased its performance when compared with other  $ePTFs$ . Both  $ePTF_{FC\_TD23}$  and  $ePTF_{WP\_TD13}$  also showed these effects when applied to the application domains AD23 and AD12, respectively. The  $\mu(RMSE)$  value of  $ePTF_{FC\_TD23}$  in the domain AD23 was as high as 7.73 (Fig. 5b), and the  $\mu(RMSE)$  value of the  $ePTF_{WP\_TD13}$  in domain AD12 was 4.57 (Fig. 6b). Both relate to the incomplete accounting for the spatial range of soil properties.

We also found that fully accounting for the spatial range of variables helps enhance the prediction capability of PTF. This finding is in line with Finke et al. (1996) and Deng et al.(2009), who suggested that the spatial structure of basic soil properties need to be fully considered to model a variable's spatial pattern. The performance of the  $ePTF_{FC\_TD11}$  degraded in the application domain of AD12 well demonstrates this point. The training samples of  $ePTF_{FC\_TD11}$  only partially represent the information on the spatial structure of the variables FC and Silt. This led to a reduced prediction capability of the  $ePTF$  when applied to a large testing domain dataset.

It was noted that the sampling resolution was found playing a minor role in regulating the uncertainty of a PTF compared to model structure (Chirico et al., 2007). This was different from our analysis. We mainly ascribed the discrepancy of the results to the different sampling strategies. That is, data samples in the work of Chirico et al. (2007, 2010) were purposely taken at spaces smaller than the correlation lengths of the observed data, and the PTF were evaluated without accounting for the effects of various spatial variograms on its prediction uncertainty (Chirico et al., 2007). In our analysis, the data samples were taken from domains of different size at different spaces, and the samples used for training the equations carried a different degree of informations about the spatial structure of the inputs. Therefore, we, believe it important to adequately address the information concerning the spatial structure of variables in training PTF, especially when applied to a large-scale prediction.

### 4.3. Is similarity/dissimilarity of soil properties important for PTF extrapolation?

One may argue that similarity/dissimilarity of soil properties was probably the dominant factor in explaining the performance of the  $ePTF$ . However, after examining the statistical difference between the soil properties, we found that similarity/dissimilarity between datasets was not responsible for the performance of the developed  $ePTF$ , probably partially because of the limited number of samples exposed to examine. Although, for instance, most of the soil properties were significantly different ( $p < 0.05$ ) between the training domain TD12 and the application domain AD12 (Table 2), the  $ePTF_{FC\_TD12}$  exhibited good performance in the application domain of AD12. Also, most of the soil properties of the domain TD11 were significantly different from those of AD11 (Table 2), and the developed  $ePTF_{FC\_TD11}$  showed satisfactory performance in the application domain AD11. In analogy, the soil properties between the training domains TD22 and TD23 were similar (See Table 2). However, the  $ePTF_{FC\_TD22}$  and  $ePTF_{FC\_TD23}$  did not present similar performances during the training stage. These all suggest that similarity/dissimilarity of soil properties is not the sole determinant of the performance of PTF extrapolation.

It should be noted that, whilst similarity/dissimilarity between datasets was found irrelevant in our analysis, it does not follow that regional or global PTF training is not meaningful. Instead, we underline that taking spatial structure into account in the training process is supplementary to similarity/dissimilarity of soil properties to derive robust  $ePTF$ . As several studies (Van Looy et al., 2017; Nemes, 2015) suggest that, it is the similarity/dissimilarity of the datasets, as well as the underlying relation of soil properties, that determine whether a PTF performs well. Therefore, we suggest that besides the first-order and second-order statistics, the underlying spatial structure of soil properties need to be considered as well.

#### 4.4. Potential influence of the spatial structure of the predicted variable

While the spatial structure of input soil properties is commonly considered, the relevance of the spatial structure of a response variable in a PTF has rarely been investigated. We previously underline the importance of adequately addressing the spatial range of explanatory variables to improve PTF prediction. However, that was meaningful only when the spatial range of the predicted variable and predictors were close each other. When their spatial ranges differed greatly, it was also worth considering the spatial range of the response variable. Two of our ensemble models (including ePTF<sub>WP,TD23</sub> and ePTF<sub>FC,TD21</sub>) may demonstrate this relevance. For example, the spatial range of both predictors of BD and OC of layer 2 was quite different from that of WP, being 109, 94, and 254 km, respectively (Table 1). The training samples of WP for training ePTF<sub>WP,TD23</sub> well characterized the spatial organization of WP. The complete information on the spatial structure of WP supported the performance of the ePTF<sub>WP,TD23</sub> in either of the application domains (See Fig. 6e), although heterogeneous samples of BD and OC were involved in training the ePTF. As such, the training domain of TD21 had a diameter of 50 km, approximately equal to the spatial range of FC. Though none of the spatial variables of layer 2 was involved as predictors of the ePTF<sub>FC,TD21</sub>, it performed best in most of the application domains AD21 and AD23 (Fig. 5e). Both ensemble models well illustrate the relevance of accounting for spatial range of a response variable in PTF development.

We underline that it might be necessary to investigate the spatial organization of a predicted variable before developing PTF. If the investigated response variable exhibits a relatively larger spatial correlation length than then predictors, it may be worth taking additional samples to address spatial variability of a response variable adequately. This would be helpful for enhancing the prediction capability of a model, irrespective of the scale of the application area. If the investigated variable had a relatively small spatial range compared to the predictors, it might be sufficient to develop robust PTF by training clustered samples within a relatively small training domain only. That would be greatly beneficial to minimize the sampling task.

#### 5. Conclusions

It is increasingly required to consider the spatial structure of input variables when training a PTF (e.g. Finke et al., 1996; Pringle et al. 2007; Deng et al., 2009; Nemes et al., 2009; Liao et al. 2011). To understand how PTF performance is influenced by considering spatial ranges of the input variables to different degree, we trained various ePTF by taking samples from a few artificially specified training domains with diameters equal to or larger than the spatial range of the input variables. We applied these ePTF to various application domains to examine their performances and robustness. Both bootstrapping and random sampling procedures were employed to address uncertainties of the ePTF predictions.

We found that for predicting FC or WP, once heterogeneous samples from outside of the spatial range of the variables interfered with the training process, the trained ePTF commonly exhibited a decreased model performance. We also found that ePTF properly accounting for spatial range of the predicted variable during the training process was conducive to improving model performance, especially when the magnitude of the spatial range of the predicted variable were considerably different from those of the predictors.

We concluded that taking additional samples from outside the spatial range of variables for training ePTF may not be favourable to enhancing its prediction capability, independent of the investigated scale. Additionally, when the magnitude of the spatial range of the predicted variable was expected to be considerably different from those of the predictors, it may be necessary to account for the spatial range of the predicted variable as well in training PTF.

#### Declaration of Competing Interest

The authors declare that they have no known competing financial interests or personal relationships that could have appeared to influence the work reported in this paper.

#### Data availability

Data will be made available on request.

#### Acknowledgements

This work was financially supported by the National Key Research and Development Program of China (Grant Number: 2022YFF1302501), and it was also partly supported by the SHUI project (Soil Hydrology research platform underpinning innovation to manage water scarcity in European and Chinese cropping systems, No. 773903) and the Tudi project (Transforming Unsustainable management of soils in key agricultural systems in EU and China. Developing an integrated platform of alternatives to reverse soil degradation, No. SEP-210648517) within the Horizon 2020 Research and Innovation Action of the European Community. The authors would like to acknowledge financial support provided by the Austrian Science Funds (FWF) as part of the Vienna Doctoral Program on Water Resource Systems (DK W1219-N28), and the TU Wien Risk network. The authors would like to thank the Editor, the Associate Editor, and the reviewers for their constructive comments that improved the manuscript.

#### Appendix A. Supplementary data

Supplementary data to this article can be found online at <https://doi.org/10.1016/j.geoderma.2023.116411>.

#### References

- Achieng, K.O., 2019. Modelling available water capacity of topsoil in a Bayesian paradigm. *Environ. Model. Softw.* 120, 104500.
- Annabi, M., Raclot, D., Bahri, H., Bailly, J.S., Gomez, C., Le Bissonnais, Y., 2017. Spatial variability of soil aggregate stability at the scale of an agricultural region in Tunisia. *Catena* 153, 157–167. <https://doi.org/10.1016/j.catena.2017.02.010>.
- Blanco, C.M.G., Gomez, V.M.B., Crespo, P., Liess, M., 2018. Spatial prediction of soil water retention in a Paramo landscape: Methodological insight into machine learning using random forest. *Geoderma* 316, 100–114.
- Bourennane, H., Lagacherie, P., Dobarco, M.R., Pasquier, C., Cousin, I., 2021. Local estimates of available water capacity and effect of measurement errors on the spatial estimates and their uncertainties. *Precis. Agric.* 22 (5), 1521–1534.
- Chirico, G.B., Medina, H., Romano, N., 2007. Uncertainty in predicting soil hydraulic properties at the hillslope scale with indirect methods. *J. Hydrol.* 334, 405–422.
- Chirico, G.B., Medina, H., Romano, N., 2010. Functional evaluation of PTF prediction uncertainty: An application at hillslope scale. *Geoderma* 155 (3–4), 193–202.
- Cichota, R., Vogeler, I., Snow, V.O., Webb, T.H., 2013. Ensemble pedotransfer functions to derive hydraulic properties for New Zealand soils. *Soil Res.* 51, 94–111.
- Deng, H.L., Ye, M., Schaap, M.G., Khaleel, R., 2009. Quantification of uncertainty in pedotransfer function-based parameter estimation for unsaturated flow modeling. *Water Resource Research* 45, W04409. <https://doi.org/10.1029/2008WR007477>, 2009.
- DeVos, B., Van Meirvenne, M., Quataert, P., Deckers, J., Muys, B., 2005. Predictive quality of pedotransfer functions for estimating bulk density of forest soils. *Soil Soc. Am. J.* 69, 500–510.
- Dobarco, M.R., Cousin, I., Le Bas, C., Martin, M.P., 2019. Pedotransfer functions for predicting available water capacity in French soils, their applicability domain and associated uncertainty. *Geoderma* 336, 81–95.
- Fatholouloumi, S., Vaezi, A.R., Alavipanah, S.K., Ghorbani, A., Biswas, A., 2020. Comparison of spectral and spatial-based approaches for mapping the local variation of soil moisture in a semi-arid mountainous area. *Sci. Total Environ.* 724, 138319.
- Finke, P.A., Wösten, J.H.M., Jansen, M.J.W., 1996. Effects of uncertainty in major input variables on simulated functional soil behaviour. *Hydrol. Process.* 10 (5), 661–669.
- Guber, A.K., Pachepsky, Y.A., van Genuchten, M.T., Simunek, J., Jacques, D., Nemes, A., Nicholson, T.J., Cady, R.E., 2009. Multimodel Simulation of Water Flow in a Field Soil Using Pedotransfer Functions. *Vadose Zone J.* 8 (1), 1–10.
- Jian, J., Shikomanov, A., Shuster, W.D., Stewart, R.D., 2021. Predicting near-saturated hydraulic conductivity in urban soils. *J. Hydrol.* 595, 126051.
- Jin, X.X., Wang, S., Yu, N., Zou, H.T., An, J., Zhang, Y.L., Wang, J.K., Zhang, Y.L., 2018. Spatial predictions of the permanent wilting point in arid and semi-arid regions of Northeast China. *J. Hydrol.* 564, 367–375.

- Kalumba, M., Bamps, B., Nyambe, I., Dondeyne, S., Van Orshoven, J., 2021. Development and functional evaluation of pedotransfer functions for soil hydraulic properties for the Zambezi River Basin. *Eur. J. Soil Sci.* 72 (4), 1559–1574.
- Liao, K.H., Xu, S.H., Wu, J.C., Ji, S.H., Lin, Q., 2011. Assessing Soil Water Retention Characteristics and Their Spatial Variability Using Pedotransfer Functions. *Pedosphere* 21 (4), 413–422.
- Liao, K.H., Xu, S., Wu, J., Zhu, Q., 2014a. Uncertainty analysis for large-scale prediction of the van Genuchten soil-water retention parameters with pedotransfer functions. *Soil Res.* 52, 431–442.
- Liao, K.H., Xua, F., Zheng, J.S., Zhu, Q., Yang, G.S., 2014b. Using different multimodel ensemble approaches to simulate soil moisture in a forest site with six traditional pedotransfer functions. *Environ. Model. Softw.* 57, 27–32.
- Ließ, M., Glaser, B., Huwe, B., 2012. Uncertainty in the spatial prediction of soil texture. Comparison of regression tree and Random Forest models. *Geoderma* 170, 70–79. <https://doi.org/10.1016/j.geoderma.2011.10.010>.
- Loiseau, T., Chen, S., Mulder, V.L., Román Dobarco, M., Richer-de-Forges, A.C., Lehmann, S., Bourennane, H., Saby, N.P.A., Martin, M.P., Vaudour, E., Gomez, C., Lagacherie, P., Arrouays, D., 2019. Satellite data integration for soil clay content modelling at a national scale. *Int. J. Appl. Earth Obs. Geoinf.* 82, 101905.
- Loosvelt, L., Pauwels, V.R.N., Cornelis, W.M., De Lannoy, G.J.M., (De Lannoy, Gabrielle J. M.) 1Verhoest, NEC (Verhoest, Niko E. C.), 2011. Impact of soil hydraulic parameter uncertainty on soil moisture modeling. *Water Resour. Res.* <https://doi.org/10.1029/2010WR009204>.
- E. Martini U. Wollschläger S. Kögler T. Behrens P. Dietrich F. Reinstorf K. Schmidt M. Weiler U. Werban S. Zacharias Spatial and Temporal Dynamics of Hillslope-Scale Soil Moisture Patterns: Characteristic States and Transition Mechanisms *Vadose Zone Journal* 14 4 2015 [vzj2014.10.0150](https://doi.org/10.1015/vzj2014.10.0150) [10.2136/vzj2014.10.0150](https://doi.org/10.2136/vzj2014.10.0150).
- Mayr, T., Jarvis, N.J., 1999. Pedotransfer functions to estimate soil water retention parameters for a modified Brooks–Corey type model. *Geoderma* 91 (1–2), 1–9.
- Milne, A.E., Lark, R.M., Addiscott, T.M., Goulding, K.W.T., Webster, C.P., O’Flaherty, S., 2005. Wavelet analysis of the scale and location-dependent correlation of modelled and measured nitrous oxide emissions from soil. *Eur. J. Soil Sci.* 56 (1), 3–17.
- Nanko, K., Ugawa, S., Hashimoto, S., Imaya, A., Kobayashi, M., Sakai, H., Ishizuka, S., Miura, S., Tanaka, N., Takahashi, M., Kaneko, S., 2014. A pedotransfer function for estimating bulk density of forest soil in Japan affected by volcanic ash. *Geoderma* 213, 36–45.
- Nemes, A., Quebedeaux, B., Timlin, D.J., 2010. Ensemble Approach to Provide Uncertainty Estimates of Soil Bulk Density. *Soil Sci. Soc. Am. J.* 74 (6), 1938–1945. <https://doi.org/10.2136/sssaj2009.0370>.
- Nemes, D.J., Timlin, Y.a., Pachepsky, A., W. J. Rawls. Evaluation of the Rawls, et al., 2009. (1982) Pedotransfer Functions for their Applicability at the U.S. National Scale. *Soil Sci. Soc. Am. J.* 73, 1638–1645. <https://doi.org/10.2136/sssaj2008.0298>.
- Parker, S.S., Seabloom, E.W., Schimel, J.P., 2012. Grassland community composition drives small-scale spatial patterns in soil properties and processes. *Geoderma* 170, 269–279. <https://doi.org/10.1016/j.geoderma.2011.11.018>.
- Pinnington, E., Amezcua, J., Cooper, E., Dadson, S., Ellis, R., Peng, J., Robinson, E., Morrison, R., Osborne, S., Quaipe, T., 2021. Improving soil moisture prediction of a high-resolution land surface model by parameterising pedotransfer functions through assimilation of SMAP satellite data. *Hydrol. Earth Syst. Sci.* 25 (3), 1617–1641.
- Pringle, M.J., Lark, R.M., 2006. Spatial analysis of the error in a model of a soil process: a case study of carbon dioxide emissions. *Vadose Zone J.* 5, 168–183.
- Pringle, M.J., Romano, N., Minasny, B., Chirico, G.B., Lark, R.M., 2007. Spatial evaluation of pedotransfer functions using wavelet analysis. *J. Hydrol.* 333 (2–4), 182–198.
- Rawls, W.J., Brakensiek, D.L., Saxton, K.E., 1982. Estimation of soil water properties. *Trans. ASAE* 25 (1316–1320), 1328.
- Schaap, M.G., 2004. Accuracy and uncertainty in PTF predictions. In: Pachepsky, Y.a., Rawls, W.J. (Eds.), *Developments in Soil Science. Development of Pedotransfer Functions in Soil Hydrology*, vol. 30. Elsevier, New York, pp. 33–43.
- Sevastas, S., Gasparatos, D., Botsis, D., Siarkos, I., Diamantaras, K.I., Bilas, G., 2018. Predicting bulk density using pedotransfer functions for soils in the Upper Anthemountas basin. Greece. *Geoderma Regional* 14 (2018), e00169.
- Sun, W.C., Yao, X.L., Cao, N., Xu, Z.X., Yu, J.S., 2016. Integration of soil hydraulic characteristics derived from pedotransfer functions into hydrological models: evaluation of its effects on simulation uncertainty. *Hydrol. Res.* 47 (5), 964–978.
- Szabo, B., Szatmari, G., Takacs, K., Laborczi, A., Mako, A., Rajkai, K., Pasztor, L., 2019. Mapping soil hydraulic properties using random-forest-based pedotransfer functions and geostatistics. *Hydrol. Earth Syst. Sci.* 23 (6), 2615–2635.
- Takagi, K., Lin, H.S., 2012. Changing controls of soil moisture spatial organization in the Shale Hills Catchment. *Geoderma* 173–174 (2012), 289–302. <https://doi.org/10.1016/j.geoderma.2011.11.003>.
- Tietje, O., Tapkenhinrichs, M., 1993. Evaluation of pedotransfer functions. *Soil Sci. Soc. Am. J.* 57, 1088–1095.
- Tromp Van Meerveld, I., McDonnell, J.J., 2006. On the interrelations between topography, soil depth, soil moisture, transpiration rates and species distribution at the hillslope scale. *Adv. Water Resour.* 29, 293–310.
- Van Looy, K., Bouma, J., Herbst, M., Koestel, J., Minasny, B., Mishra, U., Montzka, C., Nemes, A., Pachepsky, Y.A., Padarian, J., Schaap, M.G., Toth, B., Verhoef, A., Vanderborght, J., van der Ploeg, M.J., Weiermuller, L., Zacharias, S., Zhang, Y.G., Vereecken, H., 2017. Pedotransfer Functions in Earth System Science: Challenges and Perspectives. *Rev. Geophys.* 55 (4), 1199–1256.
- Winter, F., Disse, M., 2010. Saturated hydraulic conductivity from field measurements compared to pedotransfer functions in a heterogeneous arable landscape. *J. Earth Syst. Sci.* 21 (6), 923–930.
- Wösten, J.H.M., Verzandvoort, S.J.E., Leenaars, J.G.B., Hoogland, T., Wesseling, J.G., 2013. Soil hydraulic information for river basin studies in semi-arid regions. *Geoderma* 195–196, 79–86.
- Ye, M., Khaleel, R., Schaap, M.G., Zhu, J., 2007. Simulation of field injection experiments in heterogeneous unsaturated media using cokriging and artificial neural network. *Water Resour. Res.* 43, W07413. <https://doi.org/10.1029/2006WR005030>.
- Yoo, K., Amundson, R., Heimsath, A.M., Dietrich, W.E., 2006. Spatial patterns of soil organic carbon on hillslopes: Integrating geomorphic processes and the biological C cycle. *Geoderma* 130 (1–2), 47–65. <https://doi.org/10.1016/j.geoderma.2005.01.008>.
- Zhang, Y.G., Schaap, M.G., 2019. Estimation of saturated hydraulic conductivity with pedotransfer functions: A review. *J. Hydrol.* 575, 1011–1030.
- Zhang, Y.G., Schaap, M.G., Zha, Y.Y., 2018. A High-Resolution Global Map of Soil Hydraulic Properties Produced by a Hierarchical Parameterization of a Physically Based Water Retention Model. *Water Resour. Res.* 54 (2), 9774–9790.